



Effect of raw material frozen storage on physicochemical properties and flavor compounds of fermented mandarin fish (*Siniperca chuatsi*)

Yuelei Lei^{a,b}, Mingyan Ai^b, Sufang Lu^{b,*}, Hongliang Xu^b, Lan Wang^c, Jin Zhang^d, Shanbai Xiong^a, Yang Hu^{a,*}

^a College of Food Science and Technology, Huazhong Agricultural University, Wuhan 430070, China

^b Fisheries Research Institute, Wuhan Academy of Agricultural Sciences, Wuhan 430207, China

^c Institute of Agricultural Products Processing and Nuclear-Agricultural Technology, Hubei Academy of Agricultural Sciences, Wuhan 430064, China

^d Institute of Food Science, Zhejiang Academy of Agricultural Sciences, Hangzhou 310021, China

ARTICLE INFO

Keywords:

Frozen storage
Frozen mandarin fish
Fermented mandarin fish
Gas chromatography-ion mobility spectrometry
Flavor

ABSTRACT

Frozen mandarin fish (MF) is utilized for preparation fermented MF. However, how raw material (RM) affects the quality and flavor of fermented MF is unclear. This study investigated the impact and mechanism of RM frozen storage on the microstructure, texture, water distribution, and flavor of fermented MF by light microscopy, texture profile analysis, low-field nuclear magnetic resonance, gas chromatography-ion mobility spectrometry, and multivariate analysis. With increasing RM frozen storage time, both frozen MF and frozen-based fermented MF decreased in muscle fiber density while increased in muscle fiber diameter. Additionally, RM frozen storage exhibited a significant impact on the water distribution of frozen MF, while no obvious effect on that of frozen-based fermented MF. Seven odorant (2-methyl-1-propanol, 3-hydroxy-2-butanone, 2,3-butanedione, hexanal-D, ethyl acetate-D, 3-pentanone, and acetone) were shown as potential markers to distinguish fermented MF. This study could provide a theoretical basis for the production of high-quality frozen-based fermented MF.

1. Introduction

Fermented mandarin fish (*Siniperca chuatsi*, MF), a traditional fermented fish product in China, is highly popular with consumers for its unique texture and delicious flavor. Due to the periodicity of its raw supplies, many manufacturers freeze and store a large amount of fresh MF for several months in winter to ensure continuous production in the coming year. However, many producers face the challenges of what kind of freezing method is better for MF and how long it should be frozen before preparation of fermented MF. To solve these problems, it is necessary to understand the mechanisms underlying the effects of freezing methods and frozen storage on the quality and flavor of frozen and fermented MF, as well as their interactions.

Liquid nitrogen freezing (LNF), which can pass through the crystallization zone quickly and form fine crystals in aquatic products (Luo et al., 2020), is one of the best methods for batch freezing of MF.

Researchers have investigated the influence of different LNF temperatures on centrifugal loss, cooking loss, and thawing loss of Pacific oysters (Teng et al., 2023) and golden pompano (Yang et al., 2022). They found that LNF temperature could significantly affect the centrifugal loss of muscle, while had no obvious impact on cooking and thawing loss, with the optimal LNF temperature of $-80\text{ }^{\circ}\text{C}$ and $-95\text{ }^{\circ}\text{C}$ for Pacific oysters and golden pompano, respectively. Additionally, Yang et al. (2022) investigated the effect of LNF treatment on water distribution of golden pompano muscles, and LNF treatment was shown to have no significant influence on the different water components in muscle. However, as the LNF temperature declined, the relaxation time showed a downtrend, with the lowest T_{2b1} , T_{2b2} , T_{21} , and T_{22} at $-95\text{ }^{\circ}\text{C}$ (Yang et al., 2022). Moreover, Hu et al. (2021) investigated the influence of LNF and storage temperatures on the physicochemical properties, texture properties, and water distribution of Pengze crucian carp. By pre-freezing in liquid nitrogen (LN) and storage at low temperatures, the oxidative degradation

Abbreviations: RM, raw material; MF, mandarin fish; LNF, liquid nitrogen freezing; LN, liquid nitrogen; VOCs, volatile organic compounds; GC-IMS, gas chromatography-ion mobility spectrometry; LF-NMR, low-field nuclear magnetic resonance; MRI, magnetic resonance imaging; PCA, principal component analysis; HCA, hierarchical cluster analysis; PLS-DA, partial least squares discrimination analysis; VIP, variable importance in projection; VFMs, volatile flavor markers; GC-MS, gas chromatography and mass spectrometry.

* Corresponding authors.

E-mail addresses: lusufang@wuhanagri.com (S. Lu), huyang@mail.hzau.edu.cn (Y. Hu).

<https://doi.org/10.1016/j.fochx.2023.101027>

Received 16 September 2023; Received in revised form 17 November 2023; Accepted 21 November 2023

Available online 23 November 2023

2590-1575/© 2023 The Authors. Published by Elsevier Ltd. This is an open access article under the CC BY-NC-ND license (<http://creativecommons.org/licenses/by-nc-nd/4.0/>).

of Pengze crucian carp was inhibited, thawing and cooking loss was reduced, and texture was well preserved. These reports indicated that LNF and frozen storage could influence the quality of Pacific oyster, golden pompano, and Pengze crucian carp. Researchers have also examined the influence of frozen storage on volatile organic compounds (VOCs) in various fish products. By using gas chromatography-ion mobility spectrometry (GC-IMS) to analyze the influence of LNF temperatures on the VOCs of Pacific oyster, Teng et al. (2023) found that (*E*)-2-heptenal was abundant in LNF groups at -40 , -60 , and -80 °C, and at -80 °C, the LNF group could form smaller ice crystals to delay the degradation of proteins and lipids, thereby preserving the flavor substances of Pacific oyster. Additionally, Iglesias et al. (2009) evaluated the impact of frozen duration on VOCs of cultured gilthead sea bream fish. They found an increase in the concentration of hexanal, 1-penten-3-ol, 1-octen-3-ol, 2,3-octanedione, and 2,3-pentanedione during frozen storage, and revealed VOCs such as 1-octen-3-ol, 1-penten-3-ol, 4-*Z*-heptenal, and 2-octen-1-ol as potential markers to distinguish fresh and frozen fish. However, to our best knowledge, no such studies have been conducted on frozen or fermented MF.

Previous studies on fermented MF were mainly focused on flavor formation (Chen et al., 2023), microbiota (Li et al., 2013), and inoculation fermentation (Zhou et al., 2023), paying little attention to the influence of raw material (RM) frozen storage on the quality and flavor of fermented MF. The present study aimed to: 1) investigate the effects of RM frozen storage on the physicochemical characteristics of frozen MF and the corresponding fermented MF by using light microscopy, texture profile analysis, low-field nuclear magnetic resonance (LF-NMR), and multivariate analysis; 2) characterize the volatile organic compounds (VOCs) in frozen-based fermented MF by GC-IMS and chemometrics, including principal component analysis (PCA), hierarchical cluster analysis (HCA), and partial least squares discrimination analysis (PLS-DA); 3) explore the preliminary mechanism from RM to end product based on the data obtained from physicochemical characteristics and volatile flavor profile. This study may provide new insights into the influence of RM frozen storage on the quality and flavor of frozen and fermented MF.

2. Materials and methods

2.1. Preparation of frozen and fermented mandarin fish (MF)

Fresh mandarin fish (*Siniperca chuatsi*) samples were purchased at the Baishazhou Wholesale Market (Wuhan, Hubei, China) and transported alive to the lab. In the lab, after using an oxygenation device to ensure fish survival in a container with room temperature water, the fish samples were stunned to unconsciousness immediately with a wooden hammer following the methods recommended by World Organization for Animal Health (2015). Next, the samples were dissected dorsally from tail to head along the vertebrae, followed by removing the viscera and gills, washing, draining the samples completely at 4 °C for 10 min. Finally, the samples were vacuum-packed (0.1 Mpa) with food-grade polyethylene/polyamide bag (40 cm × 30 cm, thickness 0.12 mm, Wuhan Xinzhengde Plastic Co., Ltd.) and subjected to LNF at -80 °C in a LN freezer (Chengdu Kelaisi Cryogenic Equipment Co., Ltd., China) until the core temperature reached -30 °C, followed by frozen storage at -18 °C for 3 months.

Fresh MF samples were marked as R0, and fresh-based fermented MF samples were marked as F0. After thawing at 4 °C for 12 h, frozen-thawed MF samples were further analyzed, with the samples stored at -18 °C for one month, two months, and three months marked as R1, R2, and R3, and the corresponding frozen-based fermented MF samples as F1, F2, and F3, respectively. Fermented MF samples were prepared according to the traditional techniques (Li et al., 2013) for some modification by evenly coated with salt (2 % w/w), Chinese prickly ash (0.3 % w/w), chilli powder (0.3 % w/w), and sugar (0.5 % w/w). Then, MF samples were collected separately in sealed bags, loaded with twice fish

weight above each sealed bag, and then into a plastic box sealed with a cap. The MF samples were fermented at 10 °C for 7 days for further analysis.

2.2. Analysis of physical and chemical properties

2.2.1. pH and moisture content

Briefly, the minced sample (10 g) was homogenized with 100 mL distilled water for 1 min. Next, the pH value of the filtrate was determined by a pH meter (PB 10, Sartorius Lab Holding GmbH, Germany). The moisture content was measured according to direct drying method in GB 5009.3–2016 (Chinese National Standard for Determination of Moisture in Foods).

2.2.2. Thawing loss

Thawing loss was carried out according to the method of Teng et al. (2023) for some modification. Briefly, sample was thawed at 4 °C for 12 h. Thawing loss was estimated by calculating the weight of the muscle samples before (W_1) and after (W_2) thawing using equation (1):

$$\text{Thawing loss (\%)} = \frac{W_1 - W_2}{W_1} \times 100 \quad (1)$$

2.2.3. Centrifugal loss

According to the method of Teng et al. (2023) for some modification, muscle samples were weighed (W_3), wrapped with enough filter paper and centrifuged at 4000 rpm (4 °C) for 15 min. After centrifugation, the muscle samples were weighed again (W_4), and the centrifugal loss was calculated using equation (2):

$$\text{Centrifugal loss (\%)} = \frac{W_3 - W_4}{W_3} \times 100 \quad (2)$$

2.2.4. Cooking loss

Muscle samples were weighed (W_5), heated in 100 °C water bath for 10 min, and then balanced to room temperature. Next, the muscle samples were weighed again after removing the water from the surface with absorbent paper (W_6). Cooking loss was calculated by equation (3):

$$\text{Cooking loss (\%)} = \frac{W_5 - W_6}{W_5} \times 100 \quad (3)$$

2.2.5. Color measurement

The surface color of fish fillets was measured by a Minolta colorimeter (CR-10, Minolta, Osaka, Japan) in combination with a D65 light source and a 10° observer. In the CIE-lab scale, the parameters of color were expressed as L^* (brightness), a^* (redness), and b^* (yellowness). In each group, four samples were selected, and each sample was placed horizontally. The color was measured in three positions (top, middle and bottom) of the top view of the surface.

2.2.6. Hardness and adhesiveness

A TA.XT Plus Texture Analyzer (Stable Micro System, Surrey, UK) was used to evaluate the hardness and adhesiveness of muscle samples (20 mm × 20 mm × 10 mm). Texture profile analysis (TPA) was performed with a texture analyzer equipped with P/36R probe (Stable Micro System, Surrey, UK). At a constant speed of 1 mm/s, the probe was pressed downward until it reached 50 % of the sample height.

2.3. Microstructure

Samples (5 mm × 5 mm × 10 mm) collected from back muscle were sliced into 4 μm thick slices perpendicular to the orientation of muscle fibers using a pathology microtome (RM2016, Shanghai Leica Instruments Co., Ltd.). Subsequently, the sections were placed on a glass slide and stained in a hematoxylin staining solution for 8 min, and then moved to a 1 % hydrochloric acid ethanol solution to make the color

uniform. Next, the sections were stained with eosin for 3 min before washing with distilled water for 15 min. After successive dehydration in 95 % alcohol I, 95 % alcohol II, anhydrous ethanol I, and anhydrous ethanol II, as well as dewaxation in xylene I and xylene II for 5 min in each procedure, the sections were decolorized in xylene and immersed within a resin medium. Finally, each sample was observed with an optical microscope equipped with a digital camera, and the muscle fiber diameter and density were analyzed with Image-Pro Plus 6.0 software (Media Cybernetics, Inc, Rockville, MD, USA).

2.4. Low-field nuclear magnetic resonance (LF-NMR) and magnetic resonance imaging (MRI) measurements

LF-NMR and MRI measurements of muscle samples were performed with the NMI20-025 V-I NMR analyzer (Suzhou Niumag Analytical Instrument Co., Suzhou, China) as reported by Li et al. (2021) with some modification. Briefly, each sample (~5 g) was weighed into a cylindrical glass tube (25 mm × 20 cm), followed by inserting the tube into the NMR probe with the magnetic field strength of 0.55 T at 32 °C. T_2 transversal relaxation curves were measured by Carr-Purcell-Meiboom-Gill (CPMG) sequence. The raw data were fitted to multi-exponential decay curves by the MultiExp Inv Analysis software (Suzhou Niumag Analytical Instrument Co., Suzhou, China) to obtain the distribution curve of T_2 . The T_2 relaxation time and P_{T_2} (corresponding area percentage under relaxation amplitude) were recorded and calculated by curve fitting for water distribution. Three samples were used for LF-NMR relaxation analysis, and each sample was measured in triplicate. The proton density of each sample was measured by MRI using the above LF-NMR analyzer as described by Li et al. (2021) with slight modifications.

2.5. Gas chromatography-ion mobility spectrometry (GC-IMS) analysis

The VOCs of muscle samples were analyzed with GC-IMS (Favour-Spec, German Dortmund Gesellschaft für Analytische Sensorsysteme MBH (G.A.S.) following a previous method (Liu et al., 2020). The GC was equipped with a FS-SE-54-CB-1 capillary column (15 m × 0.53 mm × 1 μm), and sample (5 g) was transferred into in a 20 mL headspace vial. Automatic sampler conditions were as follows: incubation temperature was 60 °C; incubation time was 20 min; injection needle temperature was 85 °C; injection volume was 100 μL. The carrier gas followed a programmed flow: 2 mL/min for 2 min, 10 mL/min for 10 min, 100 mL/min for 20 min, and 150 mL/min for 25 min. The chromatographic column was kept at 60 °C, the IMS temperature was 45 °C, the constant flow rate was 150 mL/min, and N₂ carrier gas (purity 99.999 %) was used. All tests were repeated three times. VOCs were identified in the GC-IMS libraries by comparing standard drift time (Dt) and retention index (RI).

2.6. Statistical analysis

The analysis of variance (ANOVA) was performed using SPSS 26 (SPSS Inc., Chicago, IL, USA). Duncan multiple-range tests were used to compare differences between mean values, with a significant difference considered at $P < 0.05$. Pearson's correlation analysis, PCA, and HCA were performed based on physical and chemical indicators using the Apps in Origin 2023 (OriginLab Corp., Northampton, USA). The signal intensity data of VOCs were normalized, and the heatmap of VOCs was established using TBtools software (v1.120). Important features were identified by PLS-DA and variable importance in projection (VIP) using MetaboAnalyst 5.0 (<https://www.metaboanalyst.ca/>).

3. Results and discussion

3.1. Effects of raw material (RM) frozen storage on physicochemical properties of frozen and fermented mandarin fish (MF)

The pH of fish muscle is a helpful quality indicator. As RM frozen storage prolonged, the pH of frozen MF (R1-R3) samples increased at the early stage and then decreased, in contrast to a gradual decrease in fermented MF (F1-F3) samples (Fig. 1A). The thawing loss can measure the water loss of muscles during thawing; cooking loss can reflect the loss of liquids and water-soluble components during food heat processing; centrifugal loss can show the ability of free water and part of the immobile water to detach from muscle tissue under centrifugal force (Yang et al., 2022; Zhou et al., 2022). In this study, moisture content and thawing loss had no differences between R1-R3 samples; cooking loss was not significantly different between R1 and R2 samples, but significantly lower in R3 sample than in R0 sample; centrifugal loss was significantly higher in R1 sample relative to R0 sample, but with no significant difference between R2 and R3 samples (Fig. 1B-D). For fermented MF samples, the moisture content was significantly higher in F1-F3 samples than in F0 sample, but with no significant difference between F1-F3 samples. Additionally, F1 and F2 samples were significantly different from F0 sample in cooking loss and centrifugal loss, but without significant differences between F3 and F0 samples. Due to the rapid freezing rate of LN spray freezing, uniform and fine ice crystals were formed. During the three-month-long RM frozen storage, the thawing loss was only about 5 % for frozen MF samples, and the MF water content decreased after fermentation due to the penetration of salt into the tissue.

Hardness of fish meat is another important quality index. In Fig. 1F, it was shown that compared with fresh MF (R0) sample, frozen MF (R1-R3) samples showed a significant decrease of 18–29 % in hardness, probably due to synergistic effects between muscle fiber deformation and protein coagulation (Huang et al., 2022). However, as RM frozen storage time prolonged, the frozen MF (R1-R3) samples increased significantly in hardness, which was inconsistent with a previous study on crayfish (Huang et al., 2022). In Fig. 1G, the adhesiveness values were seen to be significantly higher in frozen MF samples (R1-R3) than in fresh MF sample (R0). However, with the increase of frozen storage time, R1-R3 samples showed no significant change in adhesiveness, agreeing with the trend of moisture content. Interestingly, the adhesiveness values in fermented MF (F1-F2) samples did not increase significantly at the early frozen stage, but decreased by 100 % in F3 versus F1 and F2 in the last frozen stage.

Color is one of the most significant quality attributes of fish products, which is directly associated with consumer preferences. During frozen storage, the L^* values had no significant differences between R1 and R2 samples. After three months of storage, the L^* of R3 samples decreased. Interestingly, the L^* in frozen-based MF was similar. In Fig. 1I, the a^* values were seen to decrease significantly during frozen storage in all frozen MF (R1-R3) samples versus fresh MF (R0) sample, but with no significant difference between R1-R3 MF samples, probably due to their vacuum packaging, allowing a slight oxidation of lipids and proteins during frozen storage. Notably, the a^* values showed no significant difference between fresh-based fermented MF (F0) and fresh MF (R0) samples, in contrast to significant differences between frozen-based fermented MF samples (F1-F3) and the corresponding frozen MF (R1-R3) samples. The redness also varied significantly in different frozen-based fermented MF (F1-F3) samples, probably due to the uneven distribution of pigments in the spices on the surface of fish samples. The variation in b^* could be associated with the oxidation of polyunsaturated fatty acids (Chen et al., 2022). In this study, the b^* was not significantly different between R0 and R2 samples, but significantly higher in R1 and R3 samples relative to R0 sample (Fig. 1J). With the extension of RM frozen storage time, the b^* of frozen MF samples increased initially and then decreased. Furthermore, the b^* showed no significant difference

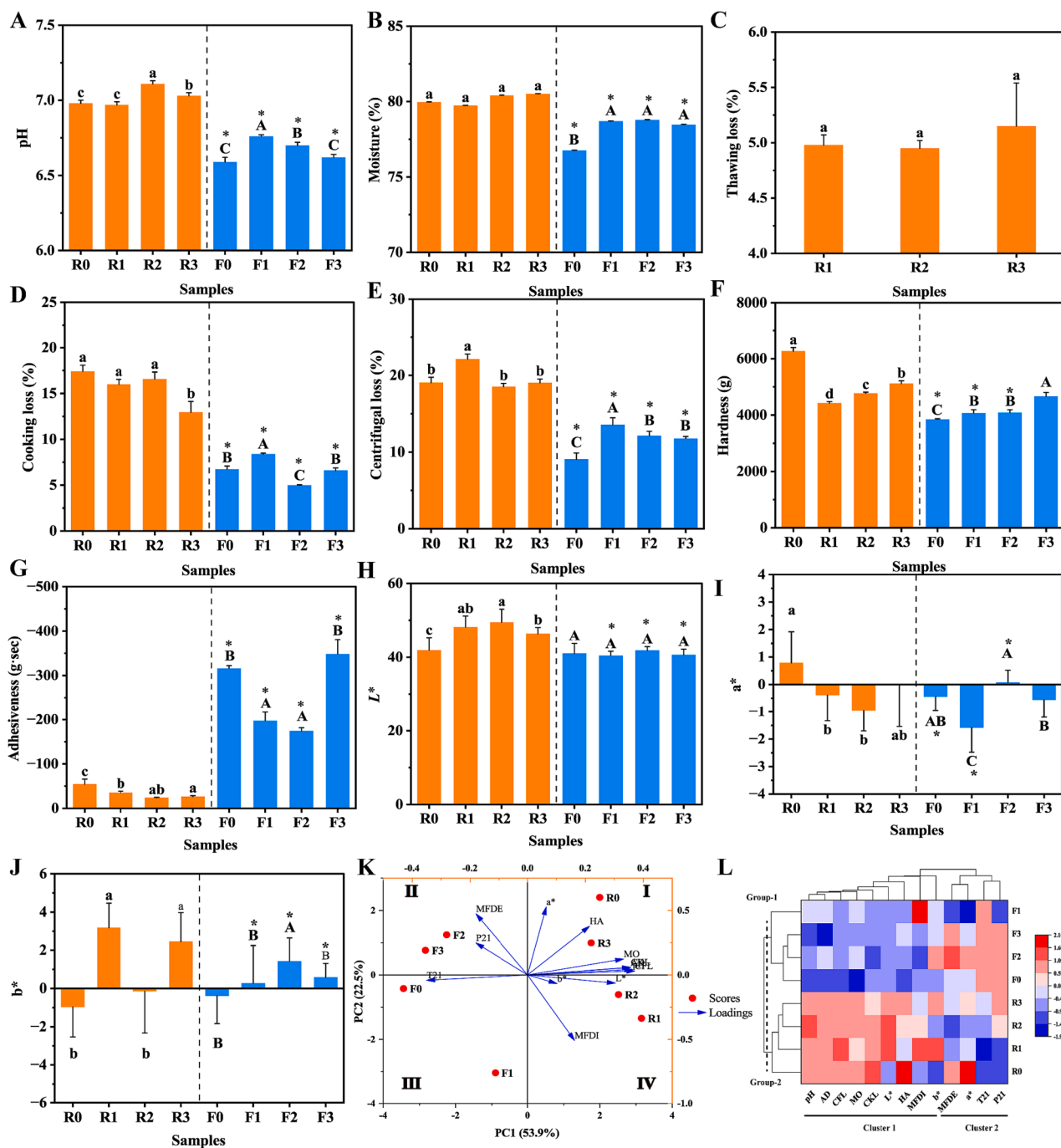


Fig. 1. pH (A), moisture content (B), thawing loss (C), cooking loss (D), centrifugal loss (E), texture (F-G), and color (H-J) of fresh, frozen and fermented MF samples. Principal component analysis (K), hierarchical cluster analysis (L) of quality indices from fresh (R0), frozen (R1-R3), and fermented (F0-F3) MF samples. Values with different lower-case letters in the columns indicate significant differences among samples of R0, R1, R2, R3 ($P < 0.05$) by Duncan's test. Values with different upper-case letters in the columns indicate significant differences among samples of F0, F1, F2, F3 ($P < 0.05$) by Duncan's test. The symbol “*” indicates significant ($P < 0.05$) differences between samples of R0 versus F0 or R1 versus F1 or R2 versus F2 or R3 versus F3 by Student's test, respectively. R0, fresh MF; R1-R3, fresh MF with liquid nitrogen spray freezing at $-80\text{ }^{\circ}\text{C}$ and stored at $-18\text{ }^{\circ}\text{C}$ for one month, two months, and three months, respectively; F0, fermented MF based on fresh MF; F1-F3, fermented MF based on one-month, two-month, and three-month frozen MF, respectively; MF, mandarin fish. CFL, centrifugal loss; CKL, cooking loss; AD, adhesiveness; HA, hardness; MFDE, muscle fiber density; MFDI, muscle fiber diameter.

between F0 and R0 samples, in contrast to significant difference between F1-F3 and R1-R3 samples. In general, RM frozen storage time had little impact on the color of frozen MF and fermented MF samples. The color difference between fermented MF and frozen MF samples was mainly caused by spices rather than frozen storage. LNF process followed by vacuum packaging was beneficial for preserving the frozen MF color and preparing the fermented MF with a stable color.

3.2. Effects of raw material (RM) frozen storage on microstructures of frozen and fermented mandarin fish (MF)

The histological images of muscle samples are shown in Fig. 2A-H. The texture of R0 tissue was clear and uniformly distributed (Fig. 2A), while R1-R3 muscle fibers were tightly connected (Fig. 2B-D), with relatively small extracellular space, and similar integrity to that of R0

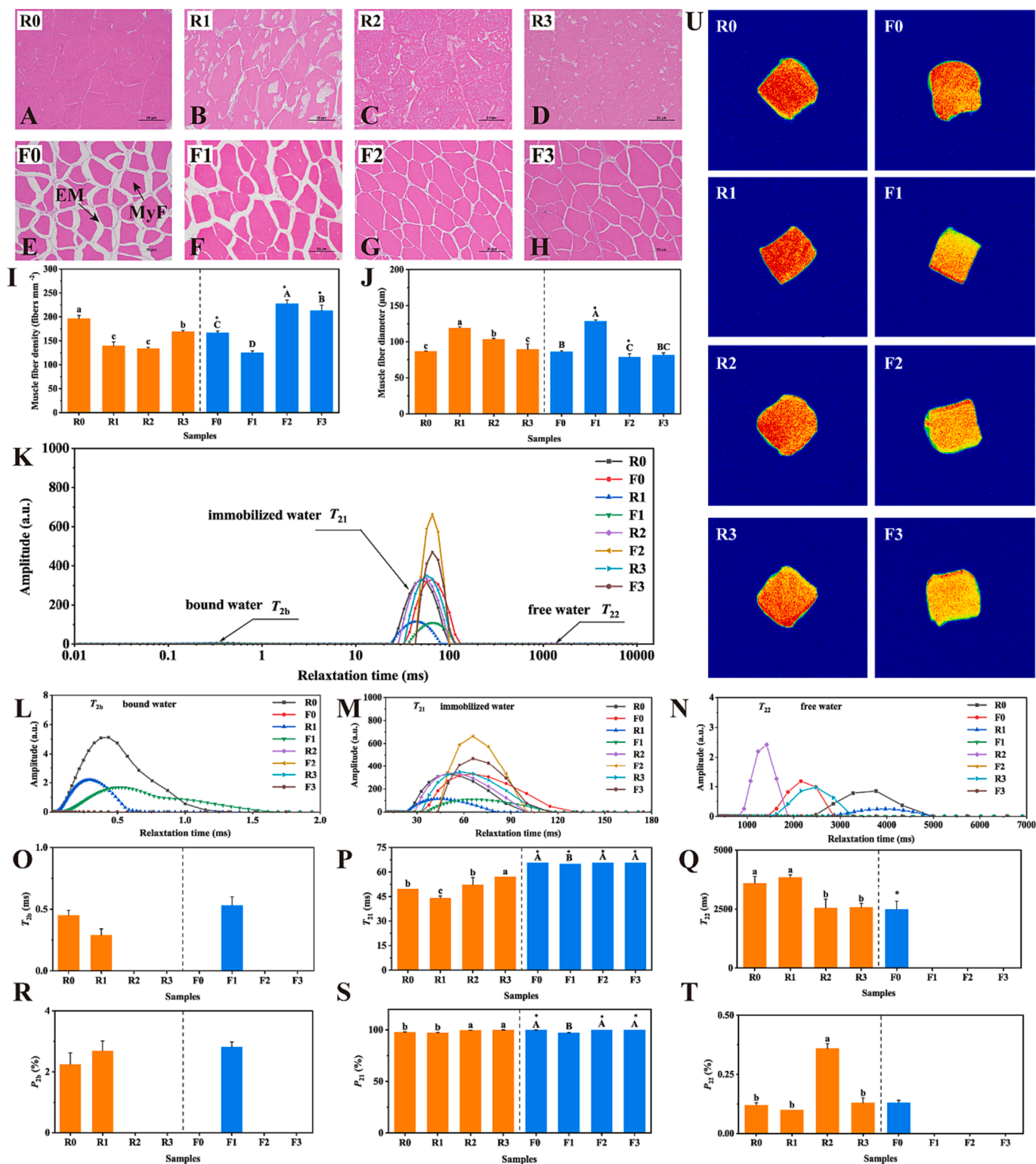


Fig. 2. Microstructure ($\times 200$) of the cross-sections based on hematoxylin and eosin (H&E) staining and light microscopy (A-H), muscle fiber density (I), and diameter (J), T_2 curve (K), T_{2b} curve (L), T_{21} curve (M), T_{22} curve (N), T_{2b} (O), T_{21} (P) and T_{22} (Q) and P_{2b} (R), P_{21} (S) and P_{22} (T) and proton density weighted images (U) of muscles from fresh (R0), frozen (R1-R3), and fermented (F0-F3) MF samples. MyF, myofibers; EM, endomysium. Scale bars = 50 μm . Values with different upper-case letter and lower-case letters in the same column indicate significant differences ($P < 0.05$). R0, fresh MF; R1-R3, fresh MF with liquid nitrogen spray freezing at -80°C and stored at -18°C for one month, two months and three months, respectively; F0, fermented MF based on fresh MF; F1-F3, fermented MF based on one-month, two-month and three-month frozen MF, respectively; MF, mandarin fish.

group. Interestingly, the texture of F0 tissue remained clear and uniform, but with a larger cell space than that of R0 tissue. The myofibers were similar between F1 and F0 samples, with a larger cellular space, while F2 (Fig. 2G) and F3 (Fig. 2H) samples had smaller cellular space than F1 sample (Fig. 2F). The muscle fiber density and diameter of different samples are shown in Fig. 2I-J. As reported by Johnston et al. (2000), firm texture was closely related to high muscle fiber density. Notably, with the extension of RM frozen storage time, the muscle fiber density of frozen MF increased (Fig. 2I), which was consistent with the trend of hardness changes in frozen MF (Fig. 1F). Moreover, the muscle fiber density of fermented MF samples also showed an uptrend. In Fig. 2J, as RM frozen storage prolonged, frozen MF (R1-R3) and fermented MF (F1-F3) samples showed a downtrend in muscle fiber diameter (Fig. 2J). Combining previous hardness indicators (Fig. 1F), the firmness of frozen and fermented MF was negatively correlated with muscle fiber diameter (Zhou et al., 2023).

3.3. Effects of raw material (RM) frozen storage on water distribution of frozen and fermented mandarin fish (MF)

The water distribution of fish muscle samples was analyzed by LF-NMR. The relaxation time distribution of T_2 is shown in Fig. 2K-N. The three water populations (T_{2b} , T_{21} , and T_{22}) were determined by relaxation time measurement. The bound water (T_{2b} , 0.1–1 ms), is the fastest relaxation population; the immobilized water (T_{21} , 40–70 ms), is the major relaxation population; the free water (T_{22} , >1000 ms), is the slower relaxation component. In Fig. 2L-N, a total of three relaxation populations were observed to be centered at 0.29–0.53 ms (T_{2b} , Fig. 2L), 44.22–65.79 ms (T_{21} , Fig. 2M), and 2493.18–3849.35 ms (T_{22} , Fig. 2N) in the present study, respectively. The T_{21} relaxation time was significantly shorter in R1 than in R0. As frozen storage time prolonged, T_{21} relaxation time increased significantly from 44.22 ms to 57.22 ms in frozen MF samples, indicating the conversion of a certain proportion of immobilized water to free water. A possible explanation for this is the formation of extracellular ice crystals during frozen storage and water redistribution, leading to mechanical damage to muscle membranes, myofibril proteins, and cellular membranes (Qi et al., 2012). Notably, T_{21} relaxation times of fermented MF (F0-F3) samples were centered at 64.97–65.79 ms with minor fluctuation. In Fig. 2P, the T_{21} relaxation times of fermented MF (F0-F3) samples were seen to increase significantly relative to the corresponding RM (R0-R3) samples, due to the addition of salt, resulting in a longer T_{21} relaxation time, as reported in a previous study on grass carp (Qin et al., 2017).

The T_{22} relaxation times of frozen MF (R1-R3) samples decreased from 3849.35 ms to 2558.76 ms during frozen storage (Fig. 2Q), probably due to less effect of protein denaturation on the free water of frozen MF in the initial frozen storage stage, while more effect with the extension of frozen storage time, leading to the absence of free water, making the bound water left in the cell less mobile. Interestingly, T_{22} disappeared in fermented MF (F1-F3) samples, indicating little or no free water in the muscle. A possible explanation is that the frozen MF lost some of its free water after thawing, and after adding salt and fermentation for up to seven days, all the remaining free water was almost lost by osmosis and pressure. This can be supported by a previous report on the disappearance of T_{22} after phosphate curing and ultrasound-assisted phosphate curing treatments in chicken breast meat (Tong et al., 2022).

P_{2b} , P_{21} and P_{22} represent the proportion of bound water (T_{2b} , Fig. 2R), immobilized water (T_{21} , Fig. 2S), and free water (T_{22} , Fig. 2T), respectively (Chen et al., 2022). In Fig. 2S, P_{21} was seen to increase from 97.21 % to 99.87 % in frozen MF (R1-R3) samples and from 97.19 % to 100 % in fermented (F1-F3) samples during frozen storage. As previously reported, salting could increase ionic strength, thus affecting water-binding ability of proteins and improving the binding water in both cellular or extracellular locations (Sigurgisladottir et al., 2000). The fresh-based fermented MF samples contained very little free water, while the frozen-based fermented MF samples contained almost no free

water or bound water, with the exception of F1 sample.

Water distribution was investigated with MRI, a nondestructive technology (Tan et al., 2021). The water distribution of fish muscle samples before (R0-R3) and after (F0-F3) fermentation was evaluated through MRI T_2 -weighted imaging (Fig. 2U), with red for a high H-proton density and blue for a low H-proton density (Wang & Xie, 2019). In Fig. 2U, R0 sample was seen to have a relatively even distribution of red color, indicating a high moisture content in the fresh samples. However, the fermented MF samples showed a yellow color with a low proton density, indicating lower moisture content in the fermented MF samples than in the fresh (R0) and frozen MF (R1-R3) samples. The tiny ice crystals formed by LNF could protect the muscle structure, retain the immobilized water (T_{21}) in the myofibrillar protein network, and stabilize the free water (T_{22}). After thawing, the free water was transferred to the fish muscle surface in the form of juice loss. When the frozen MF was fermented by dry-curing, further water loss was caused under salt penetration and gravitational maintenance. With the increase of RM frozen storage time from one month to three months, the frozen MF samples had a high proton density in the pseudo-color image, suggesting that LNF could delay water loss in frozen MF samples by quick passage through the crystallization zone to form tiny ice crystals.

3.4. Multivariate statistical analysis of muscle quality of frozen and fermented mandarin fish (MF)

3.4.1. Effects of raw material (RM) frozen storage on muscle quality of frozen and fermented mandarin fish (MF) by principal component analysis (PCA)

PCA was performed to highlight the influence of RM frozen storage duration on quality indicators of RM (R0-R3) and fermented MF (F0-F3) samples in terms of physicochemical properties (pH, moisture, centrifugal loss, cooking loss, L^* , a^* , b^* , hardness and adhesiveness), muscle microstructure (muscle fiber density and diameter), and T_2 relaxation time parameters (T_{21} and P_{21}). In Fig. 1K, the PC1 and PC2 determined by PCA were seen to describe 53.9 % and 22.5 % of the accumulative variance contribution rate, respectively, with property indicators of fresh (R0), frozen (R1-R3), and fermented (F0-F3) MF samples distributed in Quadrant I and II. Besides, the frozen MF samples had no significant difference in physical property indicators such as pH values, moisture content, centrifugal loss, cooking loss, hardness, adhesiveness, and a^* due to the clustering of these indicators in the same quadrant (Quadrant I), in contrast to a relative far distance for muscle fiber density and P_{21} (Quadrant II), T_{21} (Quadrant III), muscle fiber diameter, L^* , and b^* (Quadrant IV). The PCA results showed that fresh (R0), frozen (R1-R3), and fermented (F0-F3) MF samples could be clearly separated and distinguished in an independent space (Fig. 1K). Specifically, Fresh (R0) and frozen (R1-R3) MF samples were located on the PC1 positive axis, while fermented (F0-F3) MF samples on the PC1 negative axis, indicating a significant difference between RM (R0-R3) and fermented MF (F0-F3) samples.

3.4.2. Effects of raw material (RM) frozen storage on muscle quality of frozen and fermented mandarin fish (MF) by hierarchical cluster analysis (HCA)

The HCA heatmap of RM (R0-R3) and fermented MF (F0-F3) samples is shown in Fig. 1L. All the samples could be classified into two groups (Group (1) and Group (2)) based on the black dashed line in Fig. 1L, with Group (1) mainly for RM (R0-R3) samples and Group (2) mainly for fermented MF (F0-F3) samples. The results indicated that the quality of RMs and fermented MF products had significant differences, with fresh (R0) MF and frozen (R1-R3) MF samples distinctly differentiated in Group (2), while fresh-based (F0) fermented MF and frozen-based (F1-F3) fermented MF samples clearly distinguished in Group (1), consistent with the PCA results (Fig. 1K). Additionally, as shown in Fig. 1L, physicochemical properties of samples could be divided into two clusters (Cluster 1 and Cluster 2), with Cluster 1 including pH, centrifugal

loss, moisture, cooking loss, L^* , b^* , adhesiveness, hardness, and muscle fiber density, while Cluster 2 including a^* , muscle fiber diameter, T_{21} , and P_{21} , which represented the indicators of all samples. Cluster 1 seemed to be closely associated with WHC, color parameters, and texture properties, while Cluster 2 seemed to be closely related to water distribution. In Fig. 1L, some indicators (pH, centrifugal loss, moisture, cooking loss, and adhesiveness) were seen to be negatively correlated

with RM samples, while some indicators (pH, centrifugal loss, moisture, cooking loss, L^* , and hardness) were shown to be positively correlated with fermented MF samples.

Table 1

The signal intensities of volatile flavor compounds detected by GC-IMS in fresh MF(R0), fresh-based (F0) and frozen-based (F1-F3) fermented MF samples with PLS-DA.

Compound	VIP ^a	RI ^b	Rt ^b [sec]	Dt ^d [a.u.]	Peak intensity				
					R0	F0	F1	F2	F3
Aldehydes (10)									
Hexanal-D*	1.106 ^m	790	202.691	1.56177	162.4 ± 14.6 ^b	56.0 ± 3.2 ^c	37.4 ± 4.0 ^c	39.5 ± 12.2 ^c	217.3 ± 48.3 ^a
2-Methylbutanal-M [#]	0.568	668.3	154.257	1.15928	899.9 ± 9.1 ^a	374 ± 35.0 ^c	371.8 ± 15.6 ^c	449.4 ± 18.1 ^b	466.3 ± 9.5 ^b
Nonanal	0.513	1096.3	507.704	1.4779	628.6 ± 191.5 ^a	285.2 ± 47.1 ^b	205.5 ± 0.7 ^b	325.0 ± 46.8 ^b	266.3 ± 10.0 ^b
Hexanal-M	0.426	790.7	203.047	1.25894	496.2 ± 28.3 ^a	321.2 ± 9.2 ^b	270.0 ± 25.7 ^c	356.4 ± 27.5 ^b	502.2 ± 31.9 ^a
Heptanal	0.416	902.1	263.326	1.3283	150.1 ± 14.3 ^b	93.2 ± 11.8 ^d	116.2 ± 3.5 ^c	151.3 ± 9.4 ^b	191.3 ± 1.1 ^a
Octanal	0.373	1006.8	358.358	1.40574	96.3 ± 7.5 ^a	56.8 ± 11.7 ^b	48.6 ± 5.2 ^b	89.2 ± 11.7 ^a	61.0 ± 7.6 ^b
2-Methylbutanal-D	0.284	661	152.216	1.39728	3133.7 ± 347.2 ^a	2586.9 ± 36.4 ^b	1200.1 ± 115.5 ^c	1722.8 ± 230.6 ^d	2223.0 ± 57.2 ^c
Pentanal	0.249	694.6	162.383	1.18466	230.7 ± 18.6 ^a	143.4 ± 17.3 ^b	91.3 ± 3.5 ^c	66.1 ± 14.2 ^d	84.0 ± 4.5 ^d
3-Methylbutanal-M	0.213	647.4	148.47	1.17539	479.7 ± 33.6 ^a	322.1 ± 19.3 ^c	433.7 ± 29.5 ^{ab}	479.7 ± 40.1 ^a	413 ± 13.5 ^b
3-Methylbutanal-D	0.070	643.6	147.415	1.40375	2483.0 ± 316.6 ^{ab}	2797.3 ± 38.4 ^a	1402.4 ± 140.8 ^d	1970.8 ± 285.7 ^c	2295.0 ± 73.1 ^{bc}
Alcohols (8)									
2-Methyl-1-propanol	1.739 ^m	625.9	142.537	1.3624	41.7 ± 10.9 ^d	1118.8 ± 7.1 ^b	950.1 ± 60.4 ^c	1017.3 ± 74.0 ^c	1613.7 ± 56.3 ^a
4-Methyl-1-pentanol	0.889	834.2	225.376	1.32274	17.2 ± 2.7 ^e	52.4 ± 6.6 ^d	200.4 ± 18.7 ^a	149.1 ± 6.8 ^b	83.5 ± 6.5 ^c
3-Methylbutan-1-ol	0.653	732.7	178.254	1.48967	111.7 ± 18.5 ^d	707.8 ± 40.6 ^a	97.3 ± 2.2 ^d	603.7 ± 44.4 ^b	403.2 ± 11.3 ^c
n-Hexanol	0.467	871.2	244.425	1.32608	73.5 ± 7.5 ^e	178.5 ± 5.2 ^d	473.4 ± 14.0 ^c	842.7 ± 48.3 ^a	549.1 ± 37.6 ^b
Iso-Propanol	0.460	511.7	110.953	1.08673	59.7 ± 4.0 ^e	129.4 ± 3.7 ^d	158.9 ± 3.3 ^a	141.1 ± 1.3 ^c	149.4 ± 3.0 ^b
2,3-Butanediol	0.228	791.5	203.452	1.36397	141.0 ± 22.0 ^{bc}	103.4 ± 7.4 ^c	148.4 ± 9.9 ^b	358.6 ± 34.7 ^a	180.2 ± 20.9 ^b
1-Propanol	0.038	554.5	122.786	1.11043	855.5 ± 209.6 ^b	966.0 ± 8.2 ^b	885.2 ± 17.8 ^b	1350.0 ± 79.5 ^a	1027.5 ± 45.1 ^b
3-Octanol	0.022	993.1	338.272	1.39733	33.9 ± 5.4 ^d	52.8 ± 3.7 ^c	41.0 ± 4.6 ^d	106.9 ± 0.7 ^a	93.1 ± 5.6 ^b
Ketones (8)									
3-Hydroxy-2-butanone	1.470 ^m	724.6	174.867	1.33036	406.3 ± 29.3 ^d	4534.3 ± 51.3 ^c	9685.4 ± 275.6 ^a	6808.1 ± 337.1 ^b	7031.1 ± 266.2 ^b
2,3-Butanedione	1.321 ^m	579.8	129.794	1.16764	37.0 ± 2.6 ^c	374.4 ± 10.4 ^a	274.6 ± 8.9 ^b	270.4 ± 11.8 ^b	276.9 ± 8.8 ^b
3-Pentanone	1.084 ^m	693.5	161.894	1.35481	15.0 ± 1.2 ^d	113.0 ± 11.1 ^c	424.3 ± 17.6 ^b	474.3 ± 67.8 ^b	540.8 ± 11.5 ^a
Acetone	1.001 ^m	511.8	110.973	1.11607	297.6 ± 33.1 ^e	1154.6 ± 60.1 ^c	1782.1 ± 114.8 ^a	1458.3 ± 156.8 ^b	809.6 ± 9.0 ^d
2-Pentanone	0.629	685.5	159.007	1.36922	31.9 ± 4.4 ^e	109.4 ± 10.1 ^d	344.3 ± 27.8 ^c	587.5 ± 56.8 ^a	448.6 ± 13.7 ^b
2-Butanone-D	0.606	580.5	129.973	1.24487	376.8 ± 6.3 ^b	1062.6 ± 29.5 ^a	1074.8 ± 31.6 ^a	982 ± 177.1 ^a	1021 ± 6.6 ^c
2-Butanone-M	0.510	584.9	131.196	1.05886	791.2 ± 31.1 ^a	351.3 ± 21.3 ^d	375.2 ± 14.6 ^{cd}	407.4 ± 7.2 ^{bc}	440.8 ± 19.0 ^b
2-Heptanone	0.346	893.8	256.553	1.26037	55.1 ± 2.0 ^d	118.9 ± 4.6 ^c	169.8 ± 16.5 ^b	248.6 ± 13.6 ^a	234.9 ± 3.6 ^a
Acids (2)									
Hexanoic acid	0.233	995.8	340.538	1.30614	114.8 ± 18.1 ^a	67.6 ± 11.3 ^c	105.0 ± 23.9 ^{ab}	119.8 ± 3.3 ^a	80.7 ± 3.8 ^{bc}
Propanoic acid	0.096	766.2	192.177	1.26598	111.3 ± 22.6 ^b	103.3 ± 11.9 ^b	127.4 ± 3.5 ^b	745.8 ± 137.2 ^a	157.0 ± 9.6 ^b
Esters (2)									
Ethyl Acetate-D	1.093 ^m	611.8	138.632	1.33738	287.5 ± 59.8 ^d	2524.7 ± 148.6 ^a	1507.4 ± 153.5 ^c	2047.8 ± 228.1 ^b	2586.0 ± 46.7 ^a
Ethyl Acetate-M	0.080	605.2	136.802	1.09351	523.9 ± 56.3 ^a	489.1 ± 9.1 ^{ab}	420.2 ± 4.6 ^b	537.7 ± 62.5 ^a	489.0 ± 10.4 ^{ab}
Terpenes (14)									
(E)-Ocimene	2.024 ^m	1056.6	441.402	1.21849	71.9 ± 7.5 ^c	2521.7 ± 86.3 ^a	1510.7 ± 62.0 ^b	2527.6 ± 123.1 ^a	1562.2 ± 144.6 ^b
α-Myrcene	1.963 ^m	975.2	323.527	1.21807	69.4 ± 6.9 ^c	2437.7 ± 106 ^a	1343.3 ± 187.3 ^b	1590.4 ± 383.9 ^b	1751.3 ± 493.1 ^b
1,8-Cineole-D	1.955 ^m	1025.9	390.165	1.7262	258.4 ± 7.0 ^c	7809.9 ± 546.2 ^a	4557.0 ± 138.3 ^b	4837.6 ± 186.1 ^b	4412.6 ± 283.9 ^b
Linalool	1.655 ^m	1090.3	497.764	1.21849	100.0 ± 2.3 ^d	1817.3 ± 91.8 ^a	1032.9 ± 50.0 ^c	1613.0 ± 81.2 ^b	1036.9 ± 63.9 ^c
1,8-Cineole-M	1.649 ^m	1026.2	390.734	1.30028	814.4 ± 81.5 ^e	13384.8 ± 1132.4 ^a	11916.4 ± 158.5 ^b	6087.5 ± 116.3 ^d	10000.4 ± 496.9 ^c
2-Carene	1.518 ^m	996.8	341.524	1.21671	58.5 ± 5.1 ^c	912.0 ± 43.4 ^a	479.3 ± 63.6 ^b	534.1 ± 110.6 ^b	595.3 ± 221.0 ^b
p-Cymene	1.306 ^m	1020.2	380.702	1.21742	48.1 ± 4.9 ^c	477.2 ± 34.2 ^a	338.9 ± 21.5 ^b	265.7 ± 33.7 ^b	359.5 ± 135.8 ^{ab}
α-Thujene	1.231 ^m	925.3	282.453	1.21862	14.7 ± 1.4 ^c	114.3 ± 2.7 ^a	68.2 ± 8.0 ^b	58.5 ± 15.3 ^b	57.7 ± 20.9 ^b
α-Terpinene	1.218 ^m	1013.3	369.217	1.21742	34.9 ± 8.0 ^c	275.5 ± 32.8 ^a	133.9 ± 11.9 ^b	132.2 ± 32.4 ^b	124.4 ± 43.6 ^b
α-Pinene	1.144 ^m	932.8	288.632	1.21696	18.5 ± 3.0 ^c	124.7 ± 2.6 ^a	69.5 ± 6.8 ^b	83.5 ± 15.4 ^b	66.6 ± 44.4 ^b
β-Ocimene	1.048 ^m	1040.3	414.318	1.21304	31.0 ± 3.3 ^c	218.2 ± 30.2 ^a	137.1 ± 10.4 ^b	171.3 ± 46.9 ^{ab}	180.0 ± 67.0 ^{ab}
α-Phellandrene	0.959	1004.9	355.21	1.21887	34.9 ± 4.2 ^c	187.5 ± 21.7 ^a	100.2 ± 15.2 ^b	112.4 ± 9.0 ^b	110.2 ± 63.8 ^b
Limonene	0.782	1032.5	401.152	1.21596	35.1 ± 5.8 ^c	162.3 ± 19.5 ^{ab}	122.1 ± 12.2 ^b	211.7 ± 43.7 ^a	173.1 ± 44.3 ^{ab}
α-Fenchene	0.335	948.4	301.446	1.2159	24.4 ± 4.5 ^c	49.0 ± 0.9 ^b	52.1 ± 3.9 ^b	63.8 ± 2.1 ^a	66.4 ± 3.1 ^a

Peak intensity as mean ± standard deviation of three technical replicates.

Different lowercase letters in the same row represent significant differences by Duncan's Multiple Range Test, $P < 0.05$.

R0, fresh MF; F0, fermented MF based on fresh MF; F1, fermented MF based on one month-frozen MF; F2, fermented MF based on two months-frozen MF; F3, fermented MF based on three months-frozen MF; MF, mandarin fish.

^a RI, retention index

^b Rt, retention time in the capillary GC column

^c Dt, the drift time in the drift tube.

^m Marker volatile flavor, VIP-value > 1.

[#] the suffixes -M represents monomer.

^{*} the suffixes -D represents dimer.

3.5. Analysis of VOCs in fermented mandarin fish (MF) by GC-IMS combined with chemometrics

3.5.1. Effects of raw material (RM) frozen storage on VOCs in fermented mandarin fish (MF)

Based on the GC-IMS database, a total of 44 VOCs including their monomers (M) and dimers (D) were determined in all samples, which were 10 aldehydes, 8 ketones, 8 alcohols, 2 acids, 2 esters, and 14 terpenes (Table 1). In Fig. 3A, the flavor fingerprints provide an effective illustration to distinguish concentrations of corresponding compounds in both fresh and fermented MF samples.

As indicated in Fig. 3A, aldehydes were naturally abundant in fresh MF (Zone A, red rectangle dashed box), and after fermentation, the signal intensities of aldehydes decreased significantly, indicating that fermentation contributed largely to improving overall flavor (Fig. 3C), agreeing with a previous report that the signal intensities of these aldehydes decreased after fermentation (Wang et al., 2021). With the extension of RM frozen storage time, frozen-based fermented MF samples showed an increase in the signal intensities of 2/3-methylbutanal-D, and branched-chain aldehydes (such as 2/3-methylbutanal) were reported to be derived from Strecker degradation or microbial activity based on leucine and isoleucine (Luo et al., 2022). Interestingly, 2/3-methylbutanal had not been reported in previous studies (Li et al., 2013; Wang et al., 2021) on flavor of fermented MF by gas chromatography and mass spectrometry (GC-MS).

Microbial metabolism can produce alcohol from amino acids by decarboxylation and dehydrogenation. Some alcohols such as isopropanol, 1-propanol, 2-methyl-1-propanol, and 4-methyl-1-pentanol have a high odor threshold value and may rarely contribute to the flavor of a product. By contrast, the alcohols such as 3-methylbutan-1-ol, *n*-hexanol, 3-octanol, and 2,3-butanediol have a relatively low odor threshold value and may contribute aroma to the fermented MF. The free amino acid precursor leucine could be oxidatively deaminated to produce 3-methylbutan-1-ol with a malty aroma through Ehrlich's mechanism (Giri et al., 2010). 3-Octanol was an odorant derived from enzymatic reactions involving linolenic acid or linoleic acid with a mushroom-like aroma (Cho et al., 2006). In Fig. 3A, F0 was seen to have a stronger signal intensity of 3-methylbutan-1-ol than R0, indicating fresh MF fermentation added aroma to fermented MF. Furthermore, F2 was significantly higher than F1 and F3 in the signal intensity of 3-methylbutan-1-ol (fermented, pungent, and ethereal odor) and *n*-hexanol. The odorant *n*-hexanol (1-hexanol) had a green aroma and was derived from the oxidation of unsaturated fatty acids (Leduc et al., 2012).

Ketones have been reported to be derived from the degradation of polyunsaturated fatty acids, amino acids, and Maillard reaction and contribute to floral and fruity flavors (Luo et al., 2022; Luo et al., 2022). In Fig. 3C, the signal intensities of ketones were seen to be significantly higher in fermented MF (F0-F3) samples than in fresh (R0) sample, indicating that fermentation may contribute to increasing floral and fruity flavors. With increasing frozen storage time of RMs (R1-R3), the signal intensities of ketones in frozen-based fermented MF (F1-F3) samples showed different change trends: 1) an increase in the signal intensities of acetone and 3-hydroxy-2-butanone; 2) a decrease in the signal intensities of 3-pentanone and 3-hydroxy-2-butanone; 3) no significant changes in the signal intensities of 2-butanone-M/D and 2,3-butanedione.

Acids are mainly derived from the catabolism of amino acids or autoxidation of lipids. Two kinds of acids, including propanoic acid and hexanoic acid, were detected in all samples (Fig. 3A and Table 1). The signal intensity of hexanoic acid was higher in R0 sample than in F0 sample (Fig. 3A). Additionally, the signal intensities of hexanoic acid increased initially and then decreased in fermented MF samples as RM frozen storage time prolonged. Notably, the signal intensity of propanoic acid was higher in F2 than in the other samples. Short-chain fatty acids were found in various fish samples (An et al., 2020), contributing to sour and rancid smell.

Esters are important VOCs in fermented products. Only ethyl acetate (M and D), a contributor to fruity and sweet aroma, was identified in fresh and fermented MF samples, with no significant difference between them in the signal intensity of ethyl acetate-M (pineapple). Interestingly, the signal intensity of ethyl acetate-D (pineapple) was stronger in the fermented MF samples than in the fresh MF sample. Specifically, as frozen storage time of RMs prolonged, the frozen-based fermented MF showed significant enhancement in the signal intensity of ethyl acetate-D (pineapple) (Fig. 3A).

Terpenes are widely detected in fermented foods (Ye et al., 2022), and most of them produce pleasant floral and fruity aromas. Among the 14 terpenes detected, as shown in Fig. 3A, the signal intensities of terpenes (Area B, red dotted frame) were extremely stronger in the fermented MF samples than in the fresh MF sample. Notably, linalool and 1,8-cineole (eucalyptol, M and D) were the most abundant terpenes in all fermented MF samples. However, 1,8-cineole (mint) and linalool (floral) were possibly derived from spices during MF fermentation rather than odorants by microbial metabolism. These substances were introduced to fish for the purpose of removing off-odors, preventing spoilage, and imparting fermented products a fruity and floral aroma.

3.5.2. Effects of raw material (RM) frozen storage on VOCs of fermented mandarin fish (MF) by principal component analysis (PCA) and hierarchical cluster analysis (HCA)

The differences in VOCs between fresh, fresh-based fermented, and frozen-based fermented MF samples were revealed by PCA based on signal intensities obtained from GC-IMS (Fig. 3D). As shown in Fig. 3D, the variance contributions were 80.8 and 12.5 % for PC1 and PC2, respectively, with a cumulative variance contribution of 92.5 %. A significant distance was observed between fresh MF, fresh-based fermented MF, and frozen-based fermented MF samples. By combining GC-IMS with PCA, VOCs profiles of different samples could be clearly distinguished. A heatmap based on HCA was introduced to reveal the signal intensities of identified VOCs and their association with the effect of RM frozen storage time on fermented MF samples (Fig. 3B), with darker red zone for higher signal intensities, while darker green zone for lower signal intensities. As shown by the heatmap in Fig. 3B, R0, fresh-based fermented MF (F0), and frozen-based fermented MF (F1-F3) samples could be clearly distinguished, and so could the fermented MF (F0-F3) samples, indicating that frozen storage of RMs could affect the VOCs of fermented MF to some extent. According to cluster analysis, the 44 VOCs could be divided into five clusters (Cluster 1–5) (Fig. 3B). Fresh MF had a high level of VOCs in Cluster 3 and a low level of VOCs in Cluster 2, 4–5, while fresh-based fermented MF sample had a high level of VOCs in Cluster 1. With the extension of RM frozen storage time, the fermented MF samples had a high level of VOCs in Cluster 1 and a low level of VOCs in Cluster 2.

3.5.3. Screening of volatile flavor markers (VFMs) by partial least squares discrimination analysis (PLS-DA)

Potential volatile flavor markers (VFMs) of fresh (R0) and fermented MF (F0-F3) were investigated by PLS-DA. In the PLS-DA score plots based on GC-IMS (Fig. 4A), there was a 90 % explanation of total variance. The coefficients of R^2 (0.988) and Q^2 (0.959) above 0.5 and approaching 1.0 (Fig. 4C) were considered as satisfactory (Jin et al., 2023). After 100 cross-validations, the observed statistic *p*-value was less than 0.01 (Fig. 4D). The variable importance in projection (VIP) scores based on PLS-DA model were introduced to screen VFMs between fresh (R0) and fermented MF (F0-F3) samples (Fig. 4B). The 18 VOCs (VIP > 1) had the potential use as VFMs in GC-IMS based on PLS-DA (Fig. 4B and Table 1). As shown in Fig. 4E, 17 VFMs were negative with fresh MF samples and positive with fermented MF samples. Among the 18 potential VFMs, 11 of them were mainly derived from spices, so the other 7 VFMs (2-methyl-1-propanol, 3-hydroxy-2-butanone, 2,3-butanedione, hexanal-D, ethyl acetate-D, 3-pentanone, and acetone) could be used as key potential VFMs.

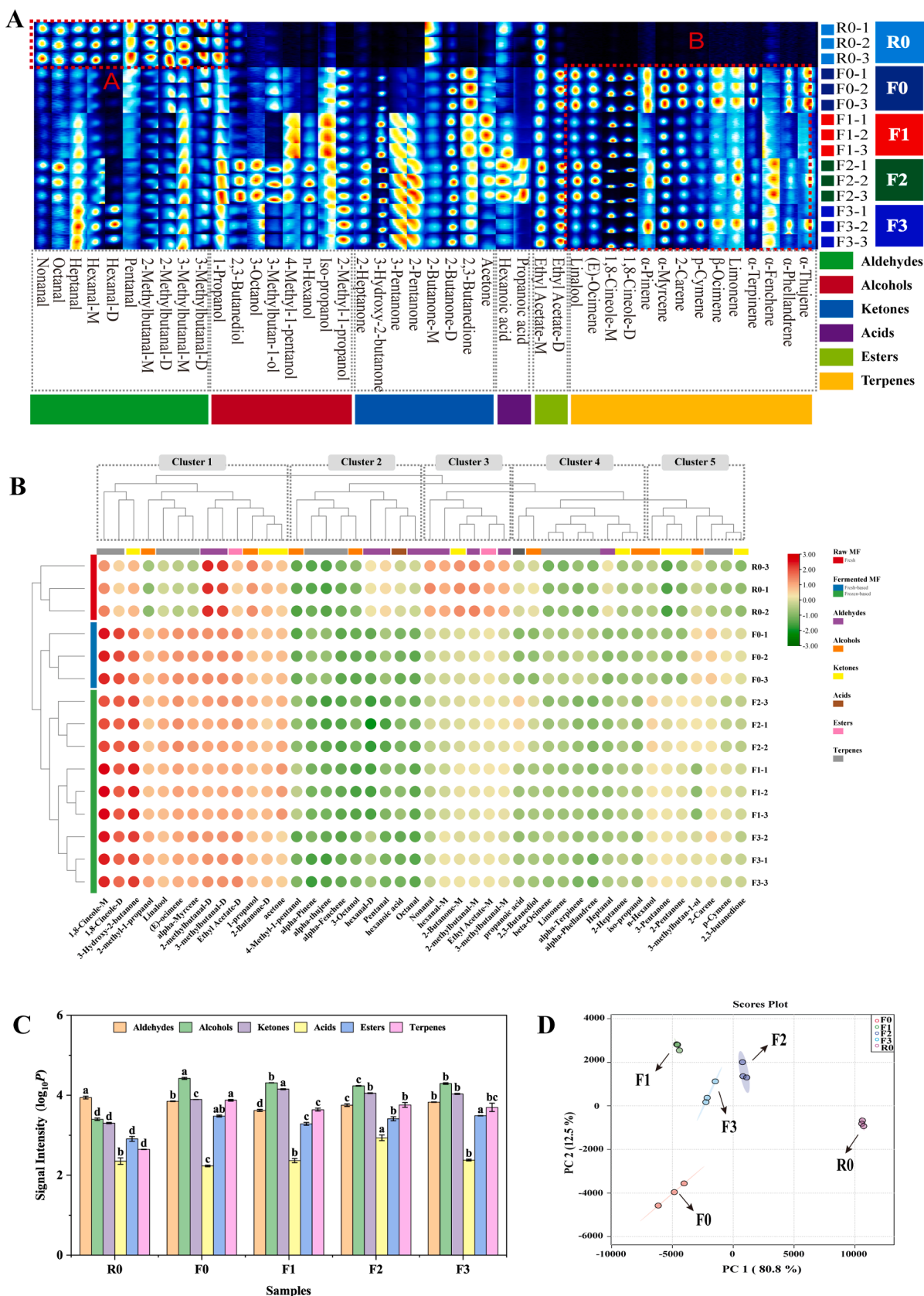


Fig. 3. Gallery plot of volatile fingerprints profiles (A), heatmap and hierarchical clustering (B), signal intensity of volatile flavor compounds (C) and PCA (D) of VOCs in fresh (R0) and fermented (F0-F3) MF samples detected by GC-IMS. Different lowercases above the error bar indicate significant differences between fresh (R0) and fermented (F0-F3) MF samples ($P < 0.05$). $\log_{10}P$ is the logarithmic value of total signal intensity for compounds of each chemical family in GC-IMS. R0, fresh MF; R1-R3, fresh MF with liquid nitrogen spray freezing at -80°C and stored at -18°C for one month, two months, and three months, respectively; F0, fermented MF based on fresh MF; F1-F3, fermented MF based on one-month, two-month and three-month frozen MF, respectively; MF, mandarin fish.

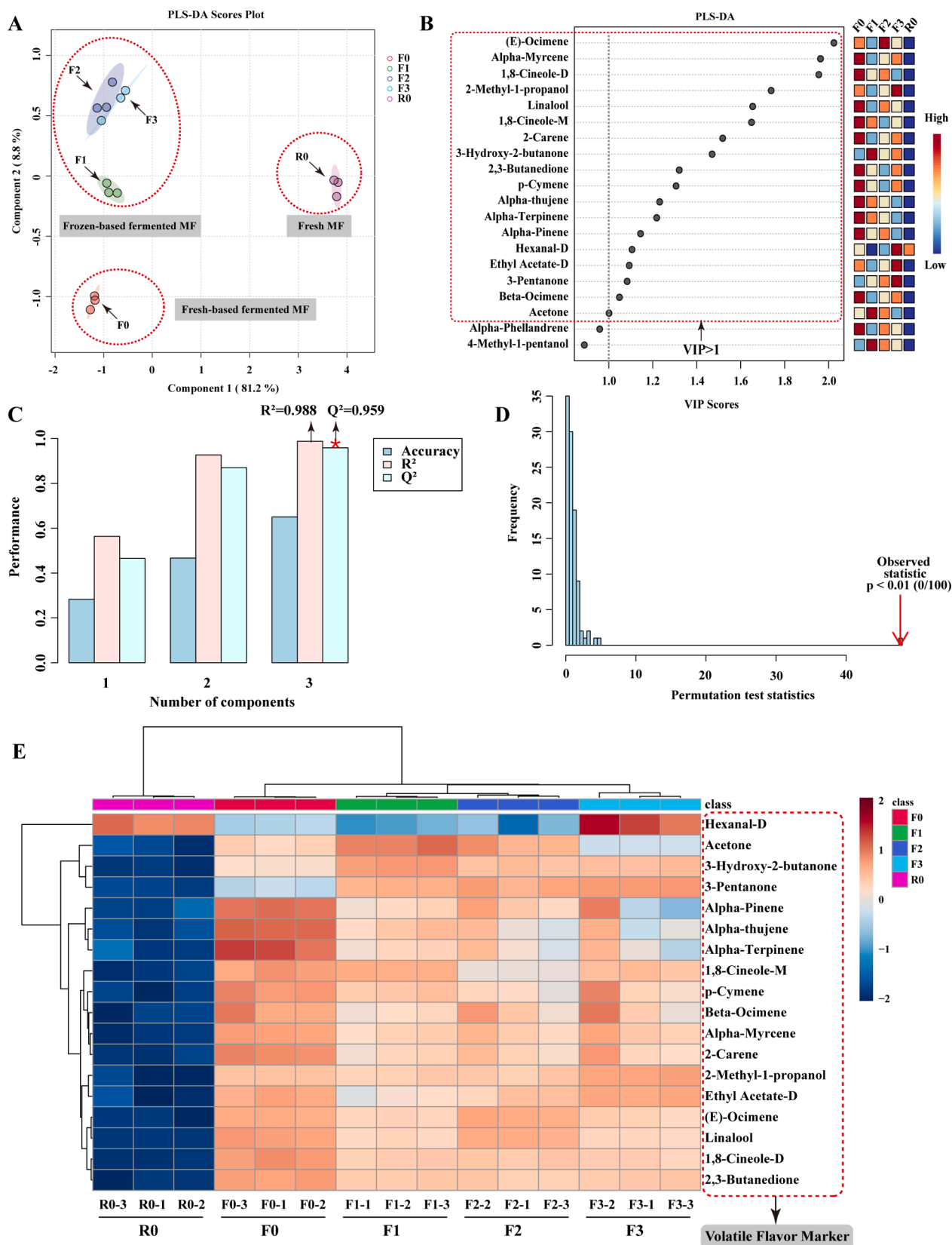


Fig. 4. PLS-DA scores plot (A) and VIP scores (B) of VOCs of fresh (R0) and fermented (F0-F3) MF samples. Cross validation (CV) with 5-fold CV (C) and permutation test under 100 times for PLS-DA (D). Heatmap of the 18 volatile flavor markers (VFM) in fresh (R0) and fermented (F0-F3) MF samples (E). R0, fresh MF; R1-R3, fresh MF with liquid nitrogen spray freezing at -80°C and stored at -18°C for one month, two months and three months, respectively; F0, fermented MF based on fresh MF; F1-F3, fermented MF based on one-month, two-month, and three-month frozen MF, respectively; MF, mandarin fish.

3.6. Preliminary mechanism exploration based on effects of raw material (RM) frozen storage on quality and VOCs of fermented mandarin fish (MF)

3.6.1. Mechanism for the influence of raw material (RM) frozen storage on quality of frozen and fermented mandarin fish (MF)

Pearson's correlation analysis was introduced to further reveal the connection between selected muscle quality indicators of frozen and

fermented MF samples, and the results are shown in heat maps in Fig. 5A and Fig. 5B, respectively. In Fig. 5A, the centrifugal loss and muscle fiber diameter of frozen MF samples were shown to have a significant negative association with moisture, hardness, adhesiveness, T_{21} , and P_{21} , while moisture, adhesiveness, and P_{21} were significantly and positively correlated with pH, hardness, adhesiveness, and T_{21} . The T_{21} and P_{21} in frozen MF samples showed a significant positive association with texture properties, indicating that water distribution can influence texture

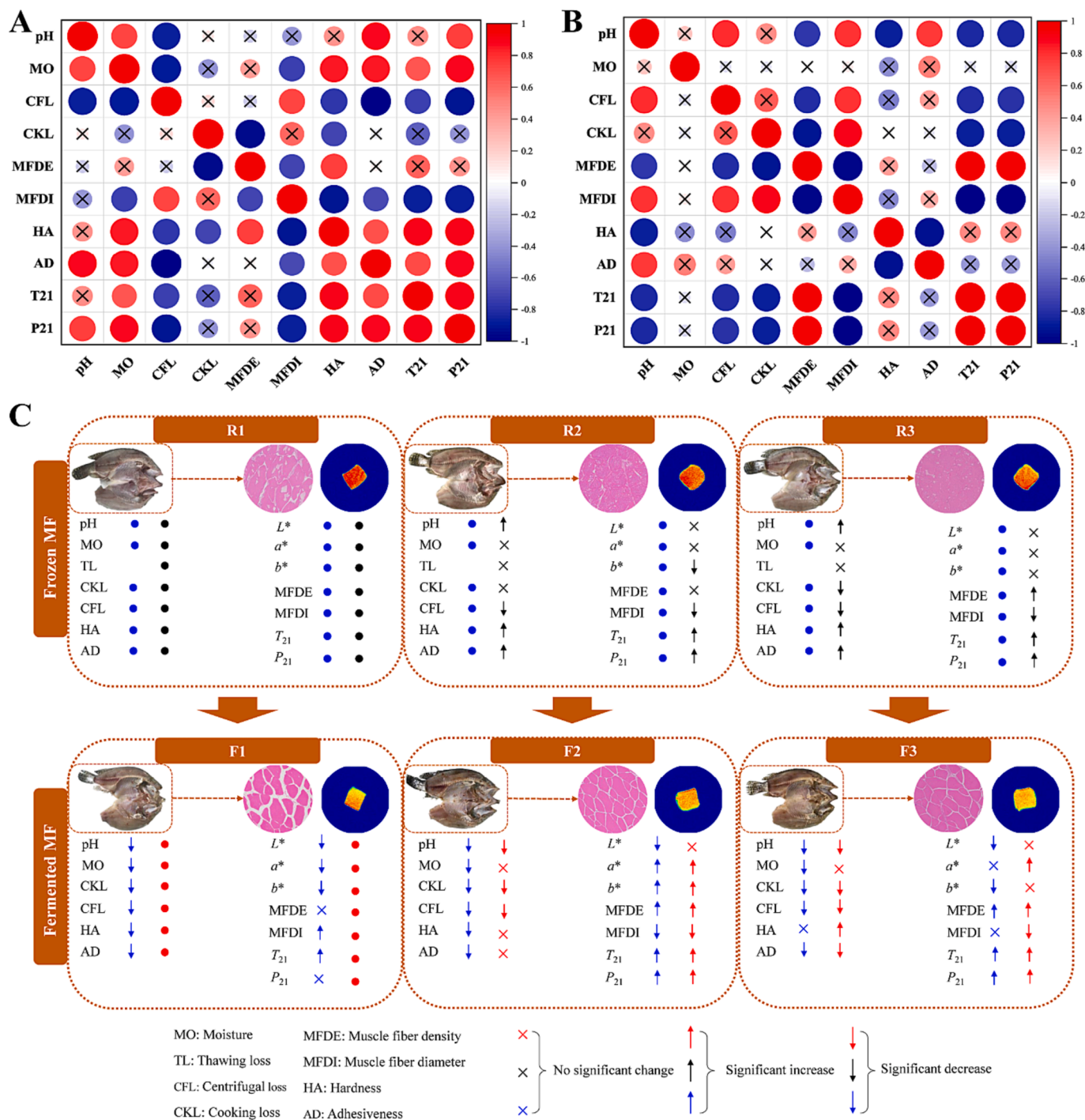


Fig. 5. Heatmap of Pearson's correlation based on quality indices from frozen MF (A) and fermented MF (B), respectively. Schematic mechanisms of the effect of frozen storage on the quality of fermented MF (C). MO, moisture; CFL, centrifugal loss; CKL, cooking loss; MFDE, muscle fiber density; MFDI, muscle fiber diameter; HA, hardness; AD, adhesiveness; T_{21} , T_{21} ; P_{21} , P_{21} . R1-R3, fresh MF with liquid nitrogen spray freezing at $-80\text{ }^{\circ}\text{C}$ and stored at $-18\text{ }^{\circ}\text{C}$ for one month, two months, and three months, respectively; F1-F3, fermented MF based on one-month, two-month, and three-month frozen MF, respectively; MF, mandarin fish.

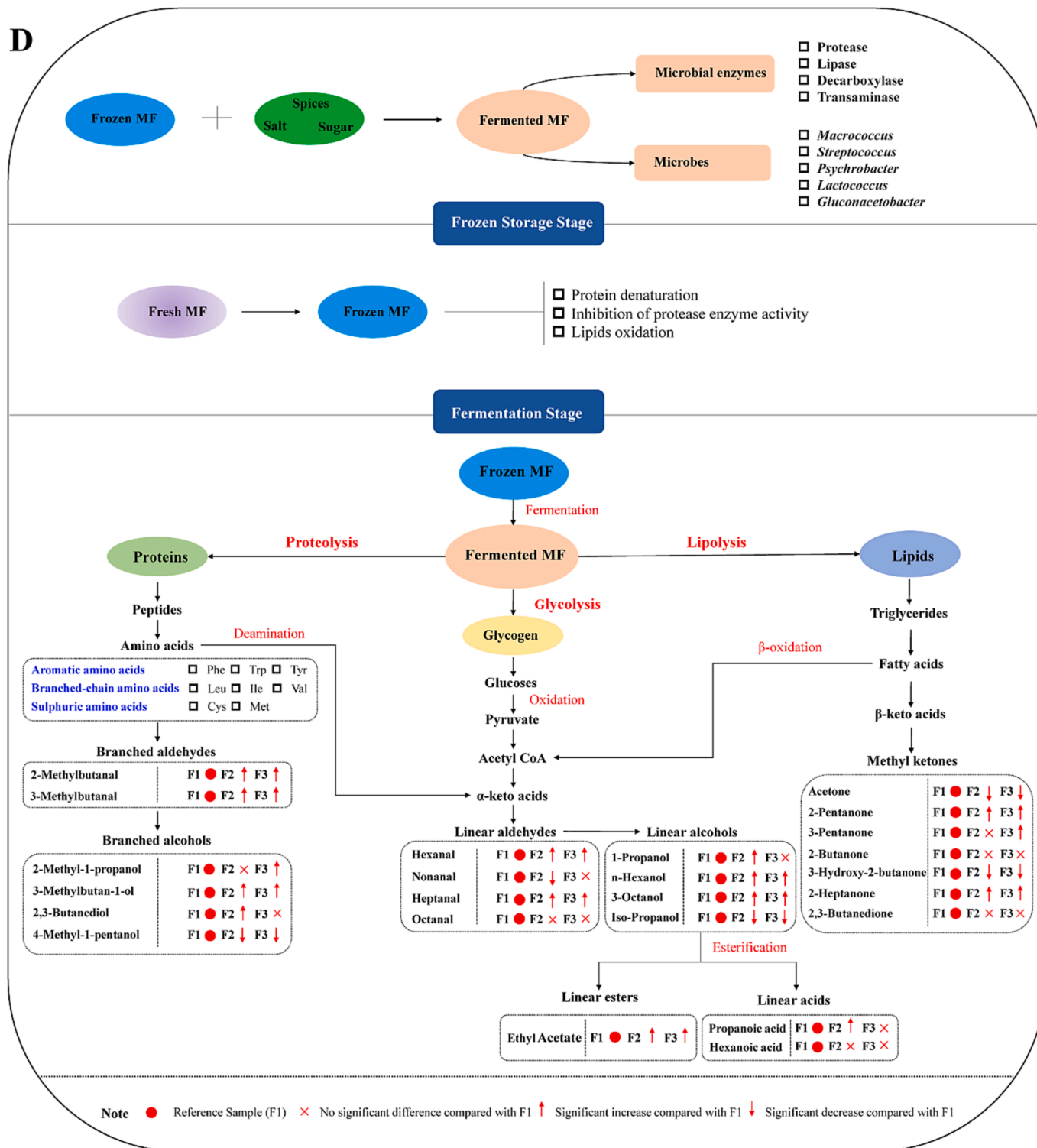


Fig. 5. (continued).

properties. In Fig. 5B, the pH, centrifugal loss, and cooking loss of fermented MF samples showed a significant negative association with muscle fiber density, T_{21} , and P_{21} , in contrast to a significant positive correlation of muscle fiber density with T_{21} and P_{21} . Correlation analysis showed a strong association between moisture distribution, muscle fiber properties, and texture properties, which is important for quality interpretation of frozen and fermented MF.

From the perspective of RM (frozen MF) to finished product (fermented MF), we proposed the possible mechanisms for the effect of RM

frozen storage on the fermented MF quality based on the data available in this study (Fig. 5). In the freezing phase, the MF was subjected to rapid LNF passage through the crystallization zone, with fine ice crystals generated in the muscle tissue. As frozen storage prolonged, the frozen MF showed a slight decrease in pH and a small loss of juice (~5%) (Fig. 1C) in muscle tissue, coupled with water redistribution and migration in muscle tissue (Fig. 2K). Besides, free water moved towards immobilized water, immobilized water became more relaxed and increased in its relative content, leading to the loss of bound water in

frozen MF. Furthermore, a decrease in muscle fiber diameter and a rise in the gap between muscle fibers caused a significant increase in hardness of frozen MF. After storage at $-18\text{ }^{\circ}\text{C}$ for three months, the frozen MF was naturally thawed at $4\text{ }^{\circ}\text{C}$ and manufactured into the corresponding fermented MF under the osmotic effect of salt and sugar, causing the water in the muscle tissue to redistribute and migrate to a varying degree again, converting almost all bound water and free water into immobilized water, with T_{21} finally around 65 ms, and an increase in water holding capacity (Fig. 1D-E). At the same time, fermented MF showed an increase in muscle fiber density (Fig. 2I) and a decrease in muscle fiber diameter (Fig. 2J), leading to the formation of a dense muscle network structure and thus an increase in hardness. Moreover, under the action of endogenous enzymes such as microorganisms, large molecules such as proteins in fish muscle formed small molecule peptides, free amino acids, etc., leading to a significant increase in muscle tissue viscosity (Fig. 1G).

3.6.2. Mechanism for the influence of raw material (RM) frozen storage on VOCs of fermented mandarin fish (MF)

Briefly, the volatile flavor development in fermented MF could be delimited into two stages (Fig. 5D): RM frozen storage stage and fermentation stage. At the RM frozen storage, LN was used to freeze fresh MF, denaturing proteins and inhibiting protease enzyme activity. Due to vacuum sealing of samples, protein denaturation was dominant and lipid oxidation was minimal at RM frozen storage. After thawing of frozen MF, protease, lipase, and microbial endogenous enzymes became more active, and fermentation became the predominant process to produce flavor.

The flavor development in fermented MF was a particularly complex process involving glycolysis (sugar metabolism), proteolysis (protein degradation), and lipolysis (lipid degradation). Fig. 5D displays the potential metabolic pathway to form some important volatiles in fermented MF. As shown in Table 1, with the extension of RM frozen storage time, frozen-based fermented MF showed an increase in the signal intensity of two branched aldehydes (2/3-methylbutanal) and one branched alcohol (2-methyl-1-propanol). Based on a previous report (Han et al., 2023), the development of fermented food flavors was based on amino acid metabolism and proteolysis. As a result of proteolysis, proteins are degraded into peptides and amino acids, which were further decomposed and deaminated to generate aromatic aldehydes or linear-chained alcohols (Fig. 5D).

In the production of aldehydes such as hexanal, heptanal, octanal, and nonanal, fatty acids are the key precursors of aroma compounds, and these compounds may have decreased signal intensities due to octanoic acid and decanoic acid transformation. As RM frozen storage time prolonged, frozen-based fermented MF showed a decrease in the signal intensity of 2 methyl ketones-type VFMs (3-hydroxy-2-butanone and acetone) (Fig. 4E and Table 1). With the degradation of lipids into fatty acids by microbes in fermented MF, methyl ketones were formed through decarboxylation. Additionally, frozen-based fermented MF exhibited an increase in the signal intensity of 1 ester-type VFM (ethyl acetate) with increasing RM frozen storage time (Fig. 4E and Table 1). Moreover, linear-chain aldehydes can be formed from microbial interactions with unsaturated fatty acids, and linear-chain alcohols can be reduced into linear-chain esters by microbes (Fig. 5D). Due to the formation of volatile compounds through complex enzymatic reactions, RMs, and non-enzymatic reactions, the influence of RM frozen storage on the flavor of frozen-based fermented MF is still worth further research, probably by integrating multi-omics techniques (Wen et al., 2023).

4. Conclusion

This study systematically explored the influence of frozen storage on physicochemical properties and volatile flavors of fermented MF from RMs to end products. Both frozen and fermented MF exhibited an

increase of myofiber density and a decrease of myofiber diameter. Additionally, T_{21} increased significantly from 44.22 ms to 57.22 ms in frozen MF while centered at 64.97–65.79 ms in fermented MF. Moreover, a total of 44 VOCs were identified in fresh, fresh-based, and frozen-based fermented MF, and 18 VIP > 1 VOCs were shown as differential volatile flavor compounds, with 7 of them (2-methyl-1-propanol, 3-hydroxy-2-butanone, 2,3-butanedione, hexanal-D, ethyl acetate-D, 3-pentanone, and acetone) as potential key VFMs to distinguish between fresh, frozen, and fermented MF. VOCs differences between fresh and frozen-based fermented MF could be visualized by GC-IMS. Furthermore, fermented MF was affected by frozen storage, due to its effect on RM microstructure, moisture distribution, and textural properties. This study provided new insights into the influence mechanism of RM frozen storage on the quality and volatile flavors of fermented MF. This study also suggested that producers should focus on the impact of RM on the quality and flavor of fermented MF and choose a proper method (such as LNF) to freeze and process it into fermented MF in a shorter time. Future studies can focus on the quality and flavor formation mechanism based on VFMs in frozen-based fermented MF through multi-omics such as metabolomics and proteomics.

CRedit authorship contribution statement

Yuelei Lei: Data curation, Formal analysis, Funding acquisition, Investigation, Methodology, Software, Writing – original draft, Resources, Visualization, Validation, Conceptualization. **Mingyan Ai:** Investigation, Data curation, Writing – review & editing. **Sufang Lu:** Funding acquisition, Project administration, Resources, Writing – review & editing. **Hongliang Xu:** Funding acquisition, Resources. **Lan Wang:** Funding acquisition, Resources. **Jin Zhang:** Formal analysis, Visualization, Software, Writing – review & editing. **Shanbai Xiong:** Project administration, Resources, Supervision, Writing – review & editing, Funding acquisition. **Yang Hu:** Conceptualization, Funding acquisition, Resources, Supervision, Validation, Writing – review & editing.

Declaration of competing interest

The authors declare that they have no known competing financial interests or personal relationships that could have appeared to influence the work reported in this paper.

Data availability

Data will be made available on request.

Acknowledgments

This work was financially supported by the National Natural Science Foundation of China (32172227), Major project of Scientific and technological R&D of Hubei Agricultural Scientific and technological Innovation Center (2020-620-000-002-03), China Agriculture Research System (CARS-46), Innovation Project of Wuhan Academy of Agricultural Sciences (CXJSFW202003-1).

References

- An, Y., Qian, Y. L., Alcazar Magana, A., Xiong, S., & Qian, M. C. (2020). Comparative characterization of aroma compounds in silver carp (*Hypophthalmichthys molitrix*), Pacific Whiting (*Merluccius productus*), and Alaska Pollock (*Theragra chalcogramma*) surimi by aroma extract dilution analysis, odor activity value, and aroma recombination studies. *Journal of Agricultural and Food Chemistry*, 68(38), 10403–10413. <https://doi.org/10.1021/acs.jafc.9b07621>
- Chen, J., Fan, Y., Zhang, X., Yuan, Z., Zhang, H., Xu, X., ... Li, C. (2022). Effect of antifreeze protein on the quality and microstructure of frozen chicken breasts. *Food Chemistry*, 134555. <https://doi.org/10.1016/j.foodchem.2022.134555>
- Chen, J.-N., Zhang, Y.-Y., Huang, X.-H., Dong, M., Dong, X.-P., Zhou, D.-Y., ... Qin, L. (2023). Integrated volatilomics and metabolomics analysis reveals the characteristic

- flavor formation in *Chouguiyu*, a traditional fermented mandarin fish of China. *Food Chemistry*, 418, Article 135874. <https://doi.org/10.1016/j.foodchem.2023.135874>
- Cho, I. H., Choi, H.-K., & Kim, Y.-S. (2006). Difference in the volatile composition of pine-mushrooms (*Tricholoma matsutake* Sing.) according to their grades. *Journal of Agricultural and Food Chemistry*, 54(13), 4820–4825. <https://doi.org/10.1021/jf0601416>
- Giri, A., Osako, K., & Ohshima, T. (2010). Identification and characterisation of headspace volatiles of fish miso, a Japanese fish meat based fermented paste, with special emphasis on effect of fish species and meat washing. *Food Chemistry*, 120(2), 621–631. <https://doi.org/10.1016/j.foodchem.2009.10.036>
- Han, J., Kong, T., Jiang, J., Zhao, X., Zhao, X., Li, P., & Gu, Q. (2023). Characteristic flavor metabolic network of fish sauce microbiota with different fermentation processes based on metagenomics. *Frontiers in Nutrition*, 10. <https://doi.org/10.3389/fnut.2023.1121310>
- Hu, Y., Zhang, N., Wang, H., Yang, Y., & Tu, Z. (2021). Effects of pre-freezing methods and storage temperatures on the qualities of crucian carp (*Carassius auratus* var. *Pengze*) during frozen storage. *Journal of Food Processing and Preservation*, 45(2). <https://doi.org/10.1111/jfpp.15139>
- Huang, J., Hu, Z., Li, G., Xiang, Y., Chen, J., & Hu, Y. (2022). Preservation mechanism of liquid nitrogen freezing on crayfish (*Procambarus clarkia*): Study on the modification effects in biochemical and structural properties. *Journal of Food Processing and Preservation*, 46(11), e17116.
- Iglesias, J., Medina, I., Bianchi, F., Careri, M., Mangia, A., & Musci, M. (2009). Study of the volatile compounds useful for the characterisation of fresh and frozen-thawed cultured gilthead sea bream fish by solid-phase microextraction gas chromatography–mass spectrometry. *Food Chemistry*, 115(4), 1473–1478. <https://doi.org/10.1016/j.foodchem.2009.01.076>
- Jin, W., Zhang, Z., Zhao, S., Liu, J., Gao, R., & Jiang, P. (2023). Characterization of volatile organic compounds of different pigmented rice after puffing based on gas chromatography-ion migration spectrometry and chemometrics. *Food Research International*, 169, Article 112879. <https://doi.org/10.1016/j.foodres.2023.112879>
- Johnston, I. A., Alderson, R., Sandham, C., Dingwall, A., Mitchell, D., Selkirk, C., ... Springate, J. (2000). Muscle fibre density in relation to the colour and texture of smoked Atlantic salmon (*Salmo salar* L.). *Aquaculture*, 189(3–4), 335–349. [https://doi.org/10.1016/S0044-8486\(00\)00373-2](https://doi.org/10.1016/S0044-8486(00)00373-2)
- Leduc, F., Tournayre, P., Kondjoyan, N., Mercier, F., Malle, P., Kol, O., ... Duflos, G. (2012). Evolution of volatile odorous compounds during the storage of European seabass (*Dicentrarchus labrax*). *Food Chemistry*, 131(4), 1304–1311. <https://doi.org/10.1016/j.foodchem.2011.09.123>
- Li, C., Wu, J., Li, Y., & Dai, Z. (2013). Identification of the aroma compounds in stinky mandarin fish (*Siniperca chuatsi*) and comparison of volatiles during fermentation and storage. *International Journal of Food Science and Technology*, 48(11), 2429–2437. <https://doi.org/10.1111/ijfs.12254>
- Li, J., Munir, S., Yu, X., Yin, T., You, J., Liu, R., ... Hu, Y. (2021). Double-crosslinked effect of TGase and EGCG on myofibrillar proteins gel based on physicochemical properties and molecular docking. *Food Chemistry*, 345, Article 128655. <https://doi.org/10.1016/j.foodchem.2020.128655>
- Liu, D., Bai, L., Feng, X., Chen, Y. P., Zhang, D., Yao, W., ... Liu, Y. (2020). Characterization of Jinhua ham aroma profiles in specific to aging time by gas chromatography-ion mobility spectrometry (GC-IMS). *Meat Science*, 168, Article 108178. <https://doi.org/10.1016/j.meatsci.2020.108178>
- Luo, X., Li, J., Yan, W., Liu, R., Yin, T., You, J., ... Hu, Y. (2020). Physicochemical changes of MTGase cross-linked surimi gels subjected to liquid nitrogen spray freezing. *International Journal of Biological Macromolecules*, 160, 642–651. <https://doi.org/10.1016/j.ijbiomac.2020.05.249>
- Luo, X., Xiao, S., Ruan, Q., Gao, Q., An, Y., Hu, Y., & Xiong, S. (2022). Differences in flavor characteristics of frozen surimi products reheated by microwave, water boiling, steaming, and frying. *Food Chemistry*, 372, Article 131260. <https://doi.org/10.1016/j.foodchem.2021.131260>
- Qi, J., Li, C., Chen, Y., Gao, F., Xu, X., & Zhou, G. (2012). Changes in meat quality of ovine longissimus dorsi muscle in response to repeated freeze and thaw. *Meat Science*, 92(4), 619–626. <https://doi.org/10.1016/j.meatsci.2012.06.009>
- Qin, N., Zhang, L., Zhang, J., Song, S., Wang, Z., Regenstein, J. M., & Luo, Y. (2017). Influence of lightly salting and sugaring on the quality and water distribution of grass carp (*Ctenopharyngodon idellus*) during super-chilled storage. *Journal of Food Engineering*, 215, 104–112. <https://doi.org/10.1016/j.jfoodeng.2017.07.011>
- Sigurðsladdottir, S., Ingvarsdóttir, H., Torrisen, O. J., Cardinal, M., & Hafsteinnsson, H. (2000). Effects of freezing/thawing on the microstructure and the texture of smoked Atlantic salmon (*Salmo salar*). *Food Research International*, 33(10), 857–865. [https://doi.org/10.1016/S0963-9969\(00\)00105-8](https://doi.org/10.1016/S0963-9969(00)00105-8)
- Tan, M., Ye, J., & Xie, J. (2021). Freezing-induced myofibrillar protein denaturation: Role of pH change and freezing rate. *LWT-Food Science and Technology*, 152, Article 112381. <https://doi.org/10.1016/j.lwt.2021.112381>
- Teng, X., Liu, Y., Chen, L., Xue, C., & Li, Z. (2023). Effects of liquid nitrogen freezing at different temperatures on the quality and flavor of Pacific oyster (*Crassostrea gigas*). *Food Chemistry*, 422, Article 136162. <https://doi.org/10.1016/j.foodchem.2023.136162>
- Tong, H., Cao, C., Du, Y., Liu, Y., & Huang, W. (2022). Ultrasonic-assisted phosphate curing: A novel approach to improve curing rate and chicken meat quality. *International Journal of Food Science and Technology*, 57(5), 2906–2917. <https://doi.org/10.1111/ijfs.15597>
- Wang, X.-Y., & Xie, J. (2019). Evaluation of water dynamics and protein changes in bigeye tuna (*Thunnus obesus*) during cold storage. *LWT-Food Science and Technology*, 108, 289–296. <https://doi.org/10.1016/j.lwt.2019.03.076>
- Wang, Y., Shen, Y., Wu, Y., Li, C., Li, L., Zhao, Y., ... Huang, H. (2021). Comparison of the microbial community and flavor compounds in fermented mandarin fish products (*Siniperca chuatsi*): Three typical types of Chinese fermented mandarin fish products. *Food Research International*, 144, Article 110365. <https://doi.org/10.1016/j.foodres.2021.110365>
- Wang, Y., Wu, Y., Shen, Y., Li, C., Zhao, Y., Qi, B., ... Chen, Y. (2021). Metabolic footprint analysis of volatile organic compounds by gas chromatography-ion mobility spectrometry to discriminate mandarin fish (*Siniperca chuatsi*) at different fermentation stages. *Frontiers in Bioengineering and Biotechnology*, 9. <https://doi.org/10.3389/fbioe.2021.805364>
- Wen, L., Yang, L., Chen, C., Li, J., Fu, J., Liu, G., ... Cao, Y. (2023). Applications of multi-omics techniques to unravel the fermentation process and the flavor formation mechanism in fermented foods. *Critical Reviews in Food Science and Nutrition*, 1–17. <https://doi.org/10.1080/10408398.2023.2199425>
- Yang, D., Li, C., Li, L., Chen, S., Hu, X., & Xiang, H. (2022). Taste mechanism of umami peptides from Chinese traditional fermented fish (*Chouguiyu*) based on molecular docking using umami receptor T1R1/T1R3. *Food Chemistry*, 389, Article 133019. <https://doi.org/10.1016/j.foodchem.2022.133019>
- Yang, Z., Liu, S., Sun, Q., Zheng, O., Wei, S., Xia, Q., ... Xu, J. (2022). Insight into muscle quality of golden pompano (*Trachinotus ovatus*) frozen with liquid nitrogen at different temperatures. *Food Chemistry*, 374, Article 131737. <https://doi.org/10.1016/j.foodchem.2021.131737>
- Ye, Z., Shang, Z., Li, M., Zhang, X., Ren, H., Hu, X., & Yi, J. (2022). Effect of ripening and variety on the physicochemical quality and flavor of fermented Chinese chili pepper (*Paojiao*). *Food Chemistry*, 368, Article 130797. <https://doi.org/10.1016/j.foodchem.2021.130797>
- Zhou, J., Dong, X., Kong, B., Sun, Q., Ji, H., & Liu, S. (2022). Effects of magnetic field-assisted immersion freezing at different magnetic field intensities on the muscle quality of golden pompano (*Trachinotus ovatus*). *Food Chemistry*, 135092. <https://doi.org/10.1016/j.foodchem.2022.135092>
- Zhou, Y., Wu, P., Jiang, W.-D., Liu, Y., Peng, Y., Kuang, S.-Y., ... Zhou, X.-Q. (2023). Dietary cinnamaldehyde improves muscle protein content by promoting muscle fiber growth via PTP1B/IGF1/PI3K/AKTs-TOR/FOXO3a signaling pathway in grass carp (*Ctenopharyngodon idella*). *Food Chemistry*, 399, Article 133799. <https://doi.org/10.1016/j.foodchem.2022.133799>
- Zhou, Y., Yang, M., Yin, J., Huang, J., Yan, Y., Zhang, F., & Xie, N. (2023). Physicochemical characteristics and gel-forming properties of mandarin fish (*Siniperca chuatsi*) protein during the fish fermentation with *Lactobacillus sake* SMF-L5: The formation of garlic-cloves shaped protein gel. *Food Chemistry*, 409, Article 135282. <https://doi.org/10.1016/j.foodchem.2022.135282>